Optica Applicata, Vol. XLIV, No. 4, 2014
DOI: 10.5277/oa140406

Investigation into spatial stochastization of an optical field scattered by nematic

PETER MAKSIMYAK, MYKHAILO GAVRYLYAK*

Correlation Optics Department, Chernivtsi University,
2 Kotsyubinsky St., Chernivtsi, 58012 Ukraine

*Corresponding author: mgavrylyak@gmail.com

This paper presents the investigation results of spatial chaotization of an optical field scattered by liquid crystals during phase transition liquid–liquid crystal under an electric field. Two stochastic parameters of the field, namely, Lyapunov's maximal index and correlation exponent were chosen for this study. It has been established that maximum variances of phase inhomogeneities of the nematic liquid crystal correspond to maximum fluctuations of an order parameter under the temperature of phase transition liquid–liquid crystal. It has been found that the analysis of the radiation field scattered during the phase transition process in the liquid–liquid crystal allows to accurately determine the phase transition temperature and voltage of forming Williams's domains.

Keywords: liquid crystal, Williams's domains, Lyapunov's maximal index, correlation exponent.

1. Introduction

In liquid crystals can occur large-scale mass flow emerges, which are accompanied by highly dynamical collective swirling and swarming motions of active particles [1, 2]. The nematic state of active matter is of particular interest, where genuine giant number fluctuations are predicted by theory and verified in experiment on driven rods [3, 4].

If you place a nematic liquid crystal (NLC) between the conductive plates then the ordered state of molecules of liquid crystal can be destroyed by voltage between the plates. This electro-optical effect was independently discovered by several experimenters, but the group of HEILMEIER understood the practical value of this discovery first [5].

The practical value of this effect is in the destruction of order placement NLC molecules, which leads to strong diffuse scattering of light and chaotization of the radiation field scattered by the liquid crystal. The general explanation for this effect is proposed by HELFRIH [6]. He explained the appearance of convective instabilities in NLC under the influence of applied field and temperature on the liquid crystal. The mechanism of formation and the evolution of spatially modulated structures are still far from under-

standing. Therefore, an important task is the investigation of the influence of temperature and applied voltage on the dynamic properties of NLC and spatial chaotization of the scattered field.

In NLC by increasing the electric field applied to the liquid crystal cell are observed crystal modes, Williams's domains and dynamic light scattering. Crystal modes are forming at low voltages (typically voltage ~1 V), molecules are oriented parallel to the electric field and liquid crystal is similar to a single crystal on its properties. Williams's domains are observed when the voltage increases to a certain critical value (about 9 V). This periodic deformation arrangement of molecules was observed by WILLIAMS [7] and was investigated by TEANEY and MIGLIORI more detailed [8]. They explained the appearance of Williams's domains by electrohydrodynamic convection in NLC under the influence of the applied field on the liquid crystal. An increase in applied voltage causes transition to a new regime. In this case Williams's domains become disordered and moving, flows of the liquid crystal become turbulent and long--range order of NLC molecules becomes completely destroyed. At the macroscopic scale, this mode leads to dynamic light scattering and the spatial chaotization of scattered radiation [9].

Electrohydrodynamic (EHD) convection in NLC has a number of properties which distinguishes it from other convective instabilities like the thermally driven Rayleigh–Bernard convection in simple fluids [10], which has been studied more intensively. Firstly, the relaxation times of such system are short owing to the small thickness of the layers in EHD convection (usually 5–200 μm). Secondly, in addition to the amplitude of the applied voltage one has the frequency and temperature as easily accessible external control parameters. This, together with the facts that the material couples strongly to an additional magnetic field and that a vast variety of NLC with different material constants are available, provides for very rich scenarios.

Theoretical models were successfully created by BODENSCHATZ *et al*. [11]. They presented essentially the full three-dimensional linear stability analysis of the basic state and a major part of the weakly-nonlinear theory of the convective state. However, the weakly-nonlinear theory is not suitable for a dynamic light scattering regime, and the influence of temperature on the process was not taken into account. The change in temperature causes the phase transition in a liquid crystal. Phase transition liquid–liquid crystal is limited in time and it belongs to the class of transition processes, which can be described by the theory of chaotic and stochastic oscillations. The coherent optical radiation scattered by a liquid crystal during phase transition also becomes chaotic [12].

In the present paper, we investigate of the influence of temperature and applied voltage on the dynamic properties of NLC and spatial chaotization of a scattered field.

2. Basic relations

The layer of NLC is the phase-inhomogeneous object, which described by the model of random phase screen (RPS) [13]. Such model assumes: infinite extension of the ob-

ject, smoothness of inhomogeneities, and phase variance less than unity. We can write the phase correlation function of NLC as

$$\psi(\rho) = \sigma^2 K(\rho) \tag{1}$$

where σ^2 is the phase variance, and $K(\rho)$ is the phase correlation coefficient.

If the phase fluctuations are statistically homogeneous and obey the Gaussian statistics, then there exists the following interrelation between the correlation characteristics of an RPS and the transverse coherence function of the field $\Gamma(\rho)$ [14, 15]:

$$\Gamma(\rho) = \exp\left\{\sigma^2\left[K(\rho) - 1\right]\right\} \tag{2}$$

Scattering of coherent radiation on liquid crystals by the action of temperature and voltage leads to time and spatial chaotization of the optical field. The theory of stochastic and chaotic oscillations [16] provides a considerable extension of conventional light-scattering techniques. We choose for this study two stochastic parameters of the field, namely, Lyapunov's maximal index λ_1 and correlation exponent ν. For experimental data, obtained at observing dynamic systems, the availability of the positive Lyapunov exponent λ_1 can be the proof of chaos existence in the system. The correlation exponent ν characterizes the complexity of such systems and determines the number of harmonics with incommensurable periods describing the subject of the study [16].

Lyapunov exponents play an important role in studying dynamic systems. They characterize the average velocity of exponential divergence of close phase trajectories. If d_0 is the initial distance between two initial points of phase trajectories, the distance between trajectories, coming off these points, in time t will be as follows:

$$d(t) = d_0 \exp(\lambda t) \tag{3}$$

The value λ is called Lyapunov exponent [17]. Each dynamic system is characterized by Lyapunov exponents spectrum λ_i ($i = 1, 2, \ldots, n$), where n is the number of differential equations which are necessary for system description. Generally speaking, a chaotic system is characterized by the divergence of phase trajectories in the similar directions and their convergence in others, *i.e.* there are both positive and negative Lyapunov exponents in the chaotic system. The sum of all the indices is negative, *i.e.*, the trajectory convergence degree exceeds that of divergence. If this condition is not fulfilled, the dynamic system is instable, and the behavior of such a system is recognized easily. Thus, in most cases, it is sufficient to calculate the largest Lyapunov exponent only. The positive value of the largest Lyapunov exponent gives the possibility of chaos existence in the system, and the value of this index characterizes chaosity intensity. We determined the largest Lyapunov exponent in optical fields using the analog interference method for measurement of the transverse correlation function [18].

To calculate the correlation dimension ν for a single generalized coordinate, namely for the object field's intensity $I(r)$, we construct the dynamic systems so that

$$I_i^{(m)} = \{I_i, I_{i+1}, \ldots, I_{i+m-1}\} \tag{4}$$

where I_i are the field intensities at the points x_i.

Then, the correlation integrals of the form

$$C_m(\varepsilon) = \lim_{N\to\infty}\left[\frac{1}{N^2}\sum_{i=1}^{N}\sum_{j=1}^{N}\Theta\left(\varepsilon - \left|\mathbf{y}_i^{(m)} - \mathbf{y}_j^{(m)}\right|\right)\right] \tag{5}$$

are evaluated. Here Θ is the Heaviside step function, N is the total number of points, $C_m(\varepsilon)$ gives the relative number of the pairs of points separated by less than ε, and m is the number of sampling points, while the numerical "distances" are given by

$$\left|I_i^{(m)} - I_j^{(m)}\right| = \left[(I_i - I_j)^2 + (I_{i+1} - I_{j+1})^2 + \ldots + (I_{i+m} - I_{j+m})^2\right]^{1/2} \tag{6}$$

For small ε, the correlation integral becomes $C(\varepsilon) \cong \varepsilon^{\nu}$. Hence, the correlation dimension is given by

$$\nu = \lim_{\varepsilon\to 0}\left[\frac{\ln[C_m(\varepsilon)]}{\ln(\varepsilon)}\right] \tag{7}$$

where m is to be increased until the slopes of $C_m(\varepsilon)$ *versus* $\ln(\varepsilon)$ curves saturate [19].

3. Experiment

We investigated spatial chaotization of an optical field scattered by a liquid crystal N8 during the phase transition liquid–liquid crystal under the action of an electric field. N8 is an eutectic mixture of MBBA and EBBA, whose structural formulas are shown in Fig. 1. Thermodynamic properties of N8 are well investigated in the temperature range of the existence of a mesomorphic phase (from 263 up to 326 K at atmospheric pressure) [20]. The layer of a liquid crystal of thickness 20 μm was placed between two glass plates with ITO.

The correlation function of the phase inhomogeneous of liquid crystal $\psi(\rho)$, Lyapunov's maximal index λ_1 and correlation exponent ν, coherent optical radiation

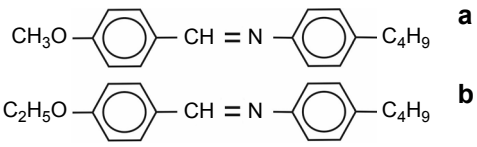

Fig. 1. The structural formulas of MBBA (**a**) and EBBA (**b**).

scattered by liquid crystal were determined from measurements of the transverse function of the coherence of field [18, 19].

The advantage of this approach for characterization of the liquid crystal is that the maximum value of the correlation function is determined by the variance of phase fluctuations (characterized by scattering ability NLC) and the half-width of the correlation function depends on the transverse scale of phase fluctuations of the liquid crystal. As for the importance of the stochastic field parameters, then λ_1 is a criterion of chaos, and ν determines the complexity of diffused field.

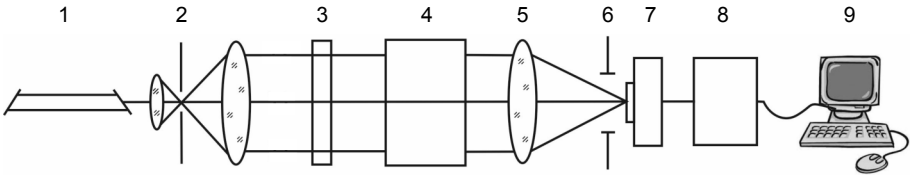

Fig. 2. Optical scheme for measurement of the transverse function of coherence of field: 1 – He-Ne laser, 2 – telescope, 3 – cell with nematic liquid crystal, 4 – transverse shear interferometer, 5 – lens, 6 – aperture, 7 – photodetector, 8 – analog-to-digital converter, 9 – personal computer.

The scheme of the experiment for measurement of the transverse function of the coherence of the field is shown in Figure 2. A single-mode He-Ne laser 1 (λ_1 = = 0.6328 μm) is used as the source of coherent optical radiation. The telescopic system 2 forms a plane wave incident on the cell 3 with NLC. Radiation scattered by the object is divided into two components of equal amplitudes by using a polarization interferometer 4. Then, the relative transversal shift of these components and collinear mixing of them at the interferometer output are provided. The objective 5 images any cross-section of the scattered field into the field-of-view diaphragm 6 and photodetector 7. The signal from the photodetector is sent through the analog to a digital converter and then to the computer 9 for further processing.

The optical scheme of the polarization interferometer 4 is shown in Fig. 3. It consists of two identical wedges 3 and 4, which form a plane-parallel plate and are situated

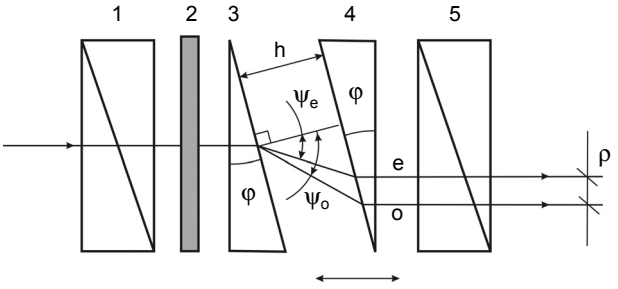

Fig. 3. Bundles path in an experimental setup interferometer.

between crossed polarizers 1 and 5. Principal optical axes of wedges 3 and 4 are parallel and form 45° angles with plane of polarization of polarizers 1 and 5. Sample 2 is situated between the polarizer 1 and the wedge 3. In Fig. 3, ordinary (o) and extraordinary (e) bundles paths in such optical scheme are shown. Space division of bundles happens on the way out from the first wedge 3.

At normal incoming bundle incidence on the wedge 3 surface, refraction angles of ordinary ψ_o and extraordinary ψ_e bundles could be written as:

$$\sin(\psi_o) = \frac{n_o}{n}\sin(\varphi), \qquad \sin(\psi_e) = \frac{n_e}{n}\sin(\varphi) \tag{8}$$

where φ – incident angle, which is equal to a prism angle; n_o and n_e – refractive indexes of ordinary and extraordinary bundles accordingly; n – refractive index of surrounding medium.

Transverse displacement between bundles ρ is assigned by the distance between wedges h and depends on the wedge angle and birefringent properties of wedge material. From the geometrical construction in Fig. 3, we can get

$$\rho = h\left[\tan(\psi_o) - \tan(\psi_e)\right]\cos(\varphi) = ah \tag{9}$$

As you see, ρ is linearly dependent only on h (parameters φ, ψ_o, ψ_e are constant for specific scheme realization). So, for a transverse displacement definition, it is necessary to know the dependence $\rho = f(h) = ah$.

In the scheme in Fig. 3, the transverse displacement ρ is accompanied by the longitudinal $\rho_{||}$, which is defined from by the following equation:

$$\rho_{||} = \left\{\left[\frac{1}{\cos(\psi_o)} - \frac{1}{\cos(\psi_e)}\right] - n_e\left[\tan(\psi_o) - \tan(\psi_e)\right]\sin(\varphi)\right\}h = bh \tag{10}$$

The longitudinal displacement between bundles in the interferometer causes the modulation of total field intensity, which dependence, while changing the distance between wedges from zero till the defined value, is represented in Fig. 3. As the longitudinal displacement between bundles is linearly bound with transverse, it is convenient to calibrate the transverse displacement with extreme values of total field intensity for longitudinal displacements (Fig. 4). The distance between extremes (maximum and minimum) amounts to $\lambda/2$. Such calibration could be provided in case of substantial scale excess of longitudinal field modulation over the transverse modulation scale.

So, even for irregular changes in the distance between wedges (Fig. 4), a transverse displacement value is known by extremes of total field intensity at the output of the interferometer. In our experiment, the distance between neighboring extremes corresponded to the transverse displacement in 3.36 μm.

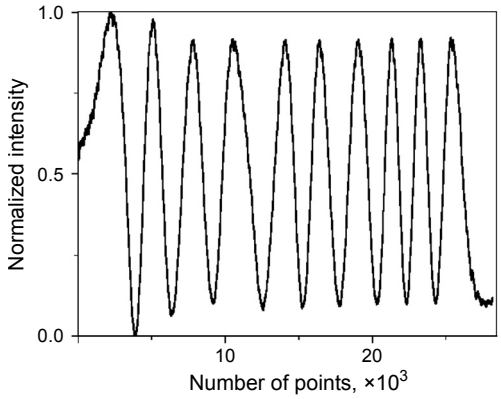

Fig. 4. Intensity changes, measured by longitudinal displacements of interferometer wedges.

From Fig. 4, the visibility of the interference pattern V was determined:

$$V = \frac{I_{\max} - I_{\min}}{I_{\max} + I_{\min}} \tag{11}$$

Here, $I_{\max}$ and $I_{\min}$ are the intensities of the resulting field for optical path differences of the mixed components $2m\lambda/2$ and $2(m + 1)\lambda/2$ (m is the integer), respectively. If the interfering beams are of equal intensities, the visibility equals to the coherence degree of the resulting field. The dependence $\Gamma(\rho)$ obtained in such a manner is used for determining a phase variance σ^2 and the phase correlation coefficient $K(\rho)$.

Two stochastic parameters of the field, namely, Lyapunov's maximal index λ_1, and correlation exponent ν, we determined from the intensity structure function $D_I(\rho)$ [18, 19, 21], which was connected with transverse coherent functions $\Gamma_\perp(\rho)$ by relation

$$D_I(\rho) = 8\Gamma_\perp(0)\left[1 - \left|\Gamma_\perp(\rho)\right|^2\right] \tag{12}$$

where $\Gamma_\perp(0)$ is the transverse coherent function for zero displacement.

4. Results and discussion

As a result of the experiment, the transverse correlation functions of phase fluctuations of the NLC depending on the temperature (the dependences for voltages 0, 6, 9 and 12 V are shown in Fig. 5) were obtained. Correlation functions show the structure dynamics of the NLC during phase transition as well as for different voltages applied to the liquid crystal cell.

When applied voltage is equal to zero, the maximal values of the correlation functions correspond to the phase transition temperature of the liquid–liquid crystal (Fig. 5).

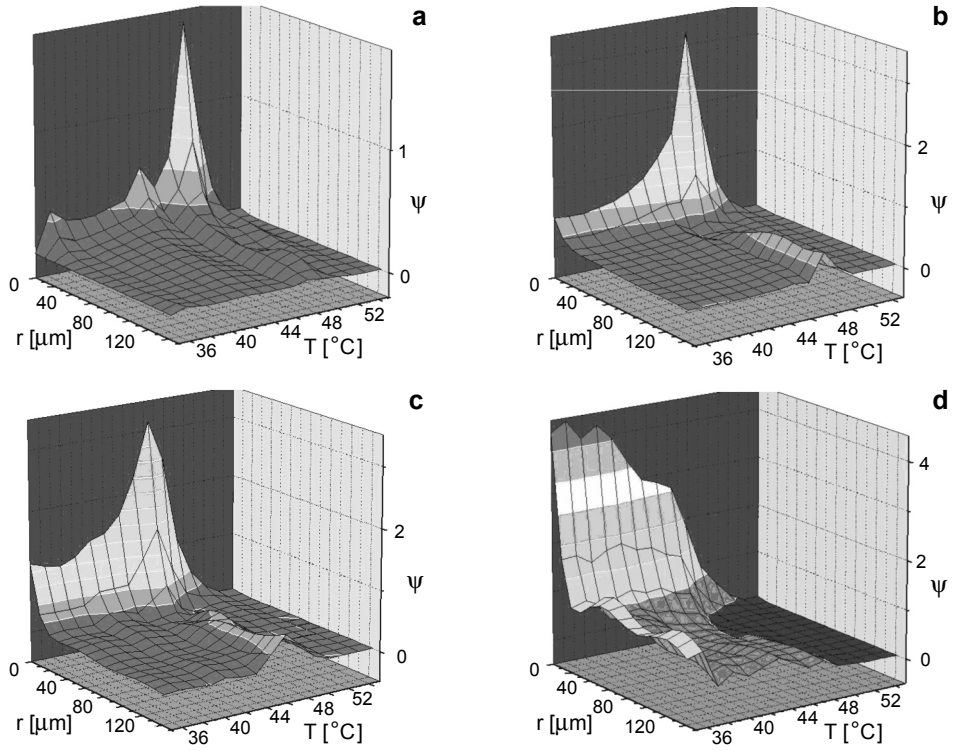

Fig. 5. The temperature dependence of the correlation function of phase at applied voltage: 0 V (**a**), 6 V (**b**), 9 V (**c**), and 15 V (**d**).

This is due to the fact that the light scattering is mainly caused by fluctuations of the orientation in NLC.

If the temperature of NLC is close to the phase transition temperature T_c, the amplitude of fluctuation increases according to the law $(T - T_c)^{-1}$. It leads to the destruction of the liquid crystal structure and chaotization of scattered radiation [22]. Voltage applied to the liquid crystal leads to convective instability and after a certain value (for our case, 9 V) to dynamic light scattering. It is shown in the form of correlation functions.

The intensity of phase fluctuations in NLC was evaluated by their variances of phase σ^2 (the maximum value of the correlation function of the phase) – Fig. 6. The variance of phase inhomogeneities in the NLC σ^2 does not change with an increase in temperature up to 45°C for voltages less than 12 V. Before the temperature of phase transition, the variances of phase inhomogeneities σ^2 sharply increase to maximum and then decrease to zero. This indicates that the maximum variance of phase inhomogeneities in the NLC corresponds to maximal fluctuations of the order parameter of the NLC and the temperature of the phase transition liquid–liquid crystal. For volt-

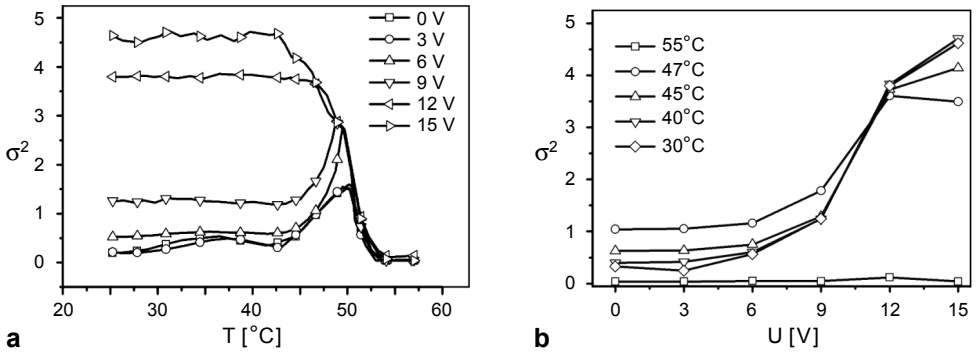

Fig. 6. The dependences of the variance of phase inhomogeneities in the nematic liquid crystal on temperature (**a**) and voltage (**b**).

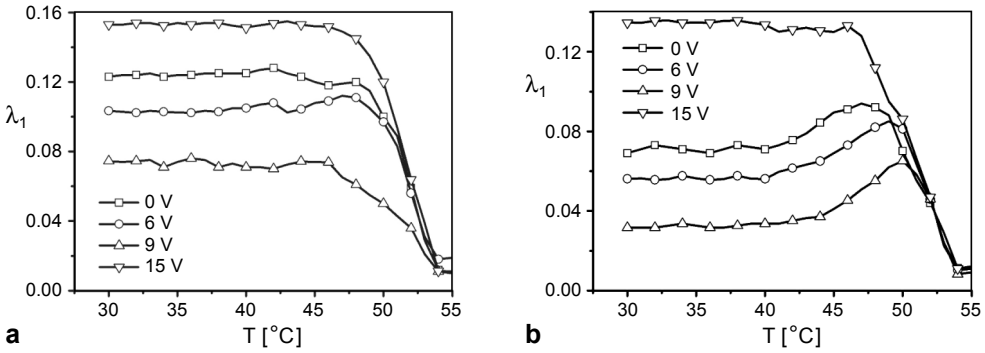

Fig. 7. The temperature dependence of Lyapunov's maximal indexes of the spatial distribution of the scattered field (**a**) and the spatial distribution of phase inhomogeneities in the nematic liquid crystal (**b**) at different voltages.

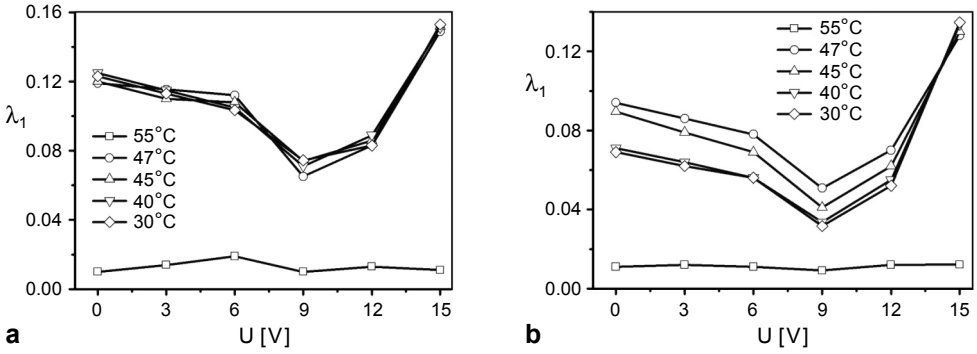

Fig. 8. The voltages dependence of Lyapunov's maximal indexes of the spatial distribution of the scattered field (**a**) and the spatial distribution of phase inhomogeneities in the nematic liquid crystal (**b**) on temperature.

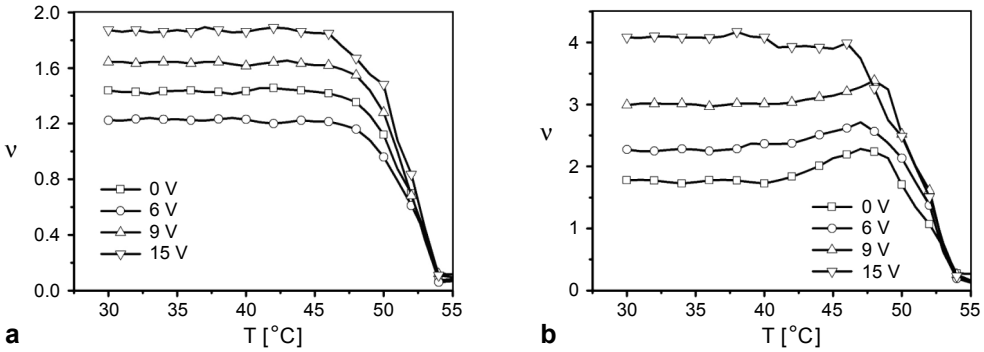

Fig. 9. The temperature dependence of the correlation exponent of the spatial distribution of the scattered field (**a**) and the spatial distribution of phase inhomogeneities in the nematic liquid crystal (**b**) at different voltages.

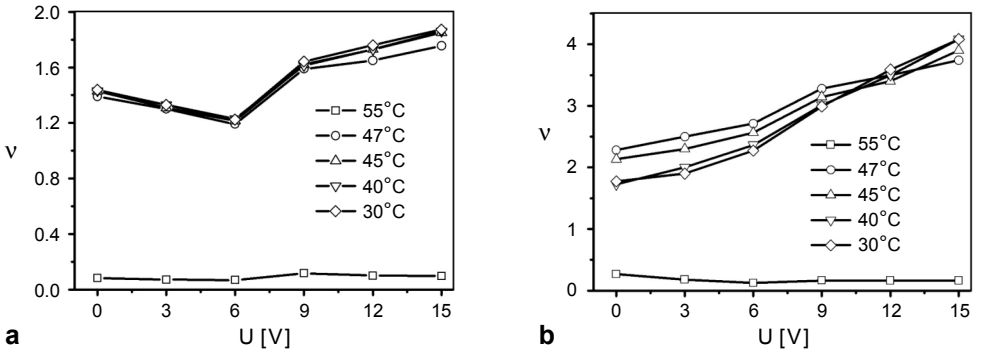

Fig. 10. The voltages dependence of the correlation exponent of the spatial distribution of the scattered field (**a**) and the spatial distribution of phase inhomogeneities in the nematic liquid crystal (**b**) on temperature.

ages higher than 12 V, the dependence of the variance phase on the temperature does not have maximum.

Lyapunov's maximal indexes (Figs. 7, 8) and correlation exponents (Figs. 9, 10) from the structure functions were calculated by the known technique [17, 18]. All temperature dependences of Lyapunov's maximal index and the correlation exponent of coordinate distributions of the scattered intensity tend to zero abruptly at the temperature of phase transition NLC–liquid. This is due to the fact that the radius of correlations decreases at the temperature phase transition, which increases the homogeneity of the near field of NLC. The radius of correlations of the isotropic phase of the liquid crystal is $r_c = r_0[T_c/(T - T_c)]^{1/2}$, where r_0 – intermolecular distance. Its value is about 5–7 Å at the isotropic phase and 50–100 Å at the point of phase transition. In the isotropic state, the threshold field is homogeneous and therefore randomness and complexity of the field go to zero.

The dependences of Lyapunov's maximal index have minimum at the voltage 9 V, which causes the Williams's domains formation. Williams's domains look like bands with spatial frequency approximately equal to the thickness of the NLC. The spatial periodicity of NLC causes reduction of the spatial chaotization in the near field. Correlation exponent does not have similar minimum. This suggests that the formation of Williams's domains does not lead to a decrease in the complexity of the scattered field. The temperature dependence of Lyapunov's maximal index and correlation exponent of the spatial distribution of phase inhomogeneities has a maximum at the temperature of phase transition (Figs. 7, 9) and the dependences of the intensity distribution of the scattered field (Figs. 9, 10) do not have a maximum.

5. Conclusions

Based on the results, we can conclude that an increase in thermal motion of molecules causes destruction of the structure of NLC at the temperature of phase transition, which is due to a decrease in the order parameter (increasing chaotization of orientation of NLC domain). In turn, this leads to greater complexity and randomization of the near field. The scattered field is a result of the coherent summation of rays from all points of NLC. As a result of the averaging of all work area of NLC, the spatial chaotization and complexity of the scattered field at the temperature of phase transition are not rising.

Thus, the analysis of the radiation field scattered during the phase transition process in the liquid–liquid crystal allows to accurately determine the phase transition temperature and voltage of forming Williams's domains. Also, the temperature of the phase transition can be determined most effectively by the maximum value of variance of phase inhomogeneities in NLC, and formation of Williams's domains is better determined by the stochastic parameters of the scattered field.

References

[1] Vicsek T., Zafeiris A., *Collective motion*, Physics Reports **517**(3–4), 2012, pp. 71–140.

[2] Marchetti M.C., Joanny J.F., Ramaswamy S., Liverpool T.B., Prost J., Madan Rao, Aditi Simha R., *Hydrodynamics of soft active matter*, Reviews of Modern Physics **85**(3), 2013, pp. 1143–1189.

[3] Narayan V., Ramaswamy S., Menon N., *Long-lived giant number fluctuations in a swarming granular nematic*, Science **317**(5834), 2007, pp. 105–108.

[4] Ramaswamy S., Aditi Simha R., Toner J., *Active nematics on a substrate: giant number fluctuations and long-time tails*, Europhysics Letters **62**(2), 2003, pp. 196–202.

[5] Heilmeier G.H., Zanoni L.A., Barton L.A., *Dynamic scattering: A new electrooptic effect in certain classes of nematic liquid crystals*, Proceedings of the IEEE **56**(7), 1968, pp. 1162–117.

[6] Helfrich W., *Conduction-induced alignment of nematic liquid crystals: basic model and stability considerations*, The Journal of Chemical Physics **51**, 1969, pp. 4092–4105.

[7] Williams R., *Domains in liquid crystals*, The Journal of Chemical Physics **39**(2), 1963, pp. 384–388.

[8] Teaney D., Migliori A., *Current- and magnetic-field-induced order and disorder in ordered nematic liquid crystals*, Journal of Applied Physics **41**(3), 1970, pp. 998–999.

[9] MURIEL M.A., MARTIN-PEREDA J.A., *Liquid-crystal electro-optic modulator based on electrohydrodynamic effects*, Optics Letters **5**(11), 1980, pp. 494–495.
[10] KAI S., *Electrohydrodynamic instability of nematic liquid crystals: growth process and influence of noise*, [In] *Noise in Nonlinear Dynamical Systems. Volume 3, Experiments and Simulations*, [Eds.] F. Moss, P.V.E. McClintock, Cambridge University Press, 1989, pp. 22–76.
[11] BODENSCHATZ E., ZIMMERMANN W., KRAMER L., *On electrically driven pattern-forming instabilities in planar nematics*, Journal de Physique France **49**(11), 11, 1988, pp. 1875–1899.
[12] GAVRYLYAK M.S., MAKSIMYAK P.P., *Stochastization of optical radiation scattered by liquid crystals*, Proceedings of SPIE **6254**, 2006, article 62541C.
[13] KONDRAT S., PONIEWIERSKI A., HARNAU L., *Orientational phase transition and the solvation force in a nematic liquid crystal confined between inhomogeneous substrates*, The European Physical Journal E **10**(2), 2003, pp. 163–170.
[14] BEKSHAEV A.YA., ANGELSKY O.V., HANSON S.G., ZENKOVA C.YU., *Scattering of inhomogeneous circularly polarized optical field and mechanical manifestation of the internal energy flows*, Physical Review A **86**(2), 2012, article 023847.
[15] ANGELSKY O.V., POLYANSKII P.V., FELDE C.V., *The emerging field of correlation optics*, Optics and Photonics News **23**(4), 2012, pp. 25–29.
[16] NEIMARK YU.I., LANDA P.S., *Stochastic and Chaotic Oscillations*, Springer, 1992, pp. 34–53.
[17] ARNOLD L., WIHSTUTZ V., *Lyapunov exponents: a survey*, [In] *Lyapunov Exponents*, [Eds.] L. Arnold, V. Wihstutz, Lecture Notes in Mathematics, Vol. 1186, 1986, pp. 1–26.
[18] GAVRYLYAK M.S., MAKSIMYAK A.P., MAKSIMYAK P.P., *Correlation method for measuring the largest Lyapunov exponent in optical fields*, Ukrainian Journal of Physical Optics **9**(2), 2008, pp. 119–127.
[19] ANGELSKY O.V., MAKSIMYAK P.P., PERUN T.O., *Optical correlation method for measuring spatial complexity in optical fields*, Optics Letters **18**(2), 1993, pp. 90–92.
[20] BOGDANOV D.L., GHEVORKYAN E.V., LAGUNOV A.S., *Acoustical properties of liquid crystals in a rotating magnetic field*, Akusticheskij Zhurnal **26**(1), 1980, pp. 28–34.
[21] ANGELSKY O.V., USHENKO A.G., BURKOVETS D.N., USHENKO YU.A., *Polarization visualization and selection of biotissue image two-layer scattering medium*, Journal of Biomedical Optics **10**(1), 2005, article 014010.
[22] FRIED F., GURTIN M.E., *Continuum theory of thermally induced phase transitions based on an order parameter*, Physica D: Nonlinear Phenomena **68**(3–4), 1993, pp. 326–343.

Received June 5, 2014